Supporting Information

S1. XRD patterns of YAG samples with different reaction time, different solvents and different al

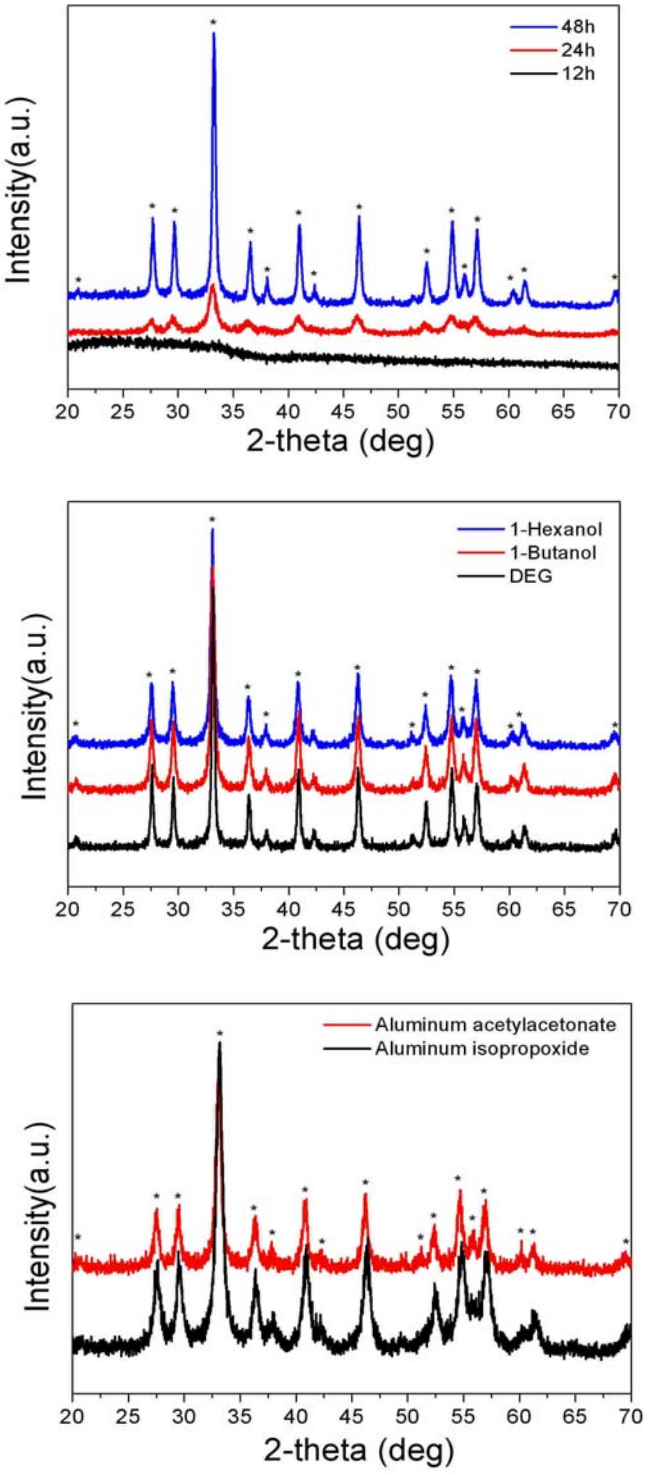

Figure S1: XRD patterns of YAG samples with different reaction time, different solvents and different aluminum source.

S2. EDX measurements of YAG:Ce1% and YAG:Ce6% samples.

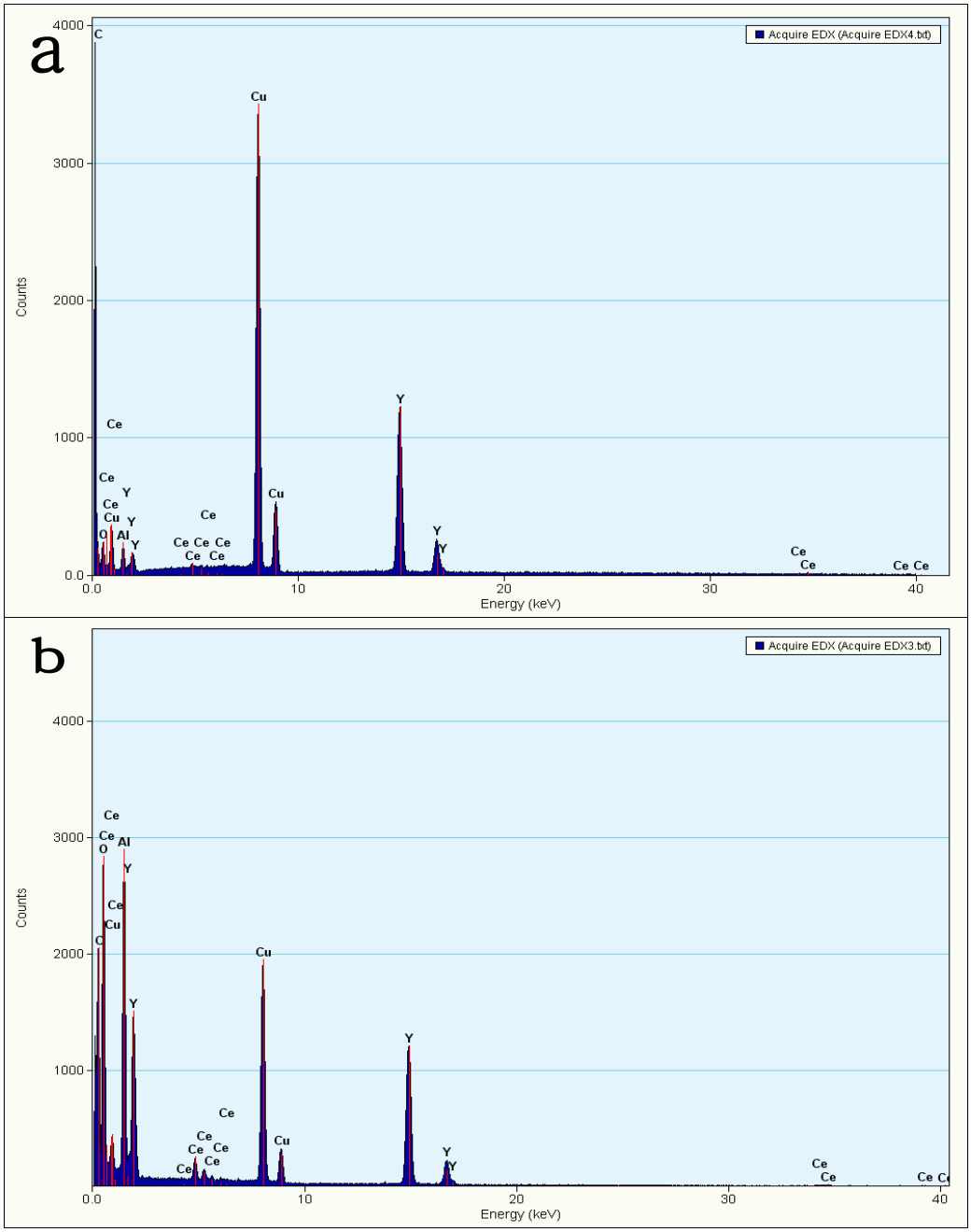

Figure S2: EDX spectra of YAG:Ce1%(a) and YAG:Ce6%(b) nanoparticles.

S3. FTIR patterns of YAG samples obtained with a substitution of DEG by 1-hexanol and 1-butanol. When DEG was replaced by 1-hexanol and 1-butanol, the YAG can also formed and no variation can be observed in the FTIR spectrum. The results indicate that the 1,4-BD plays an important role in the crystal formation.

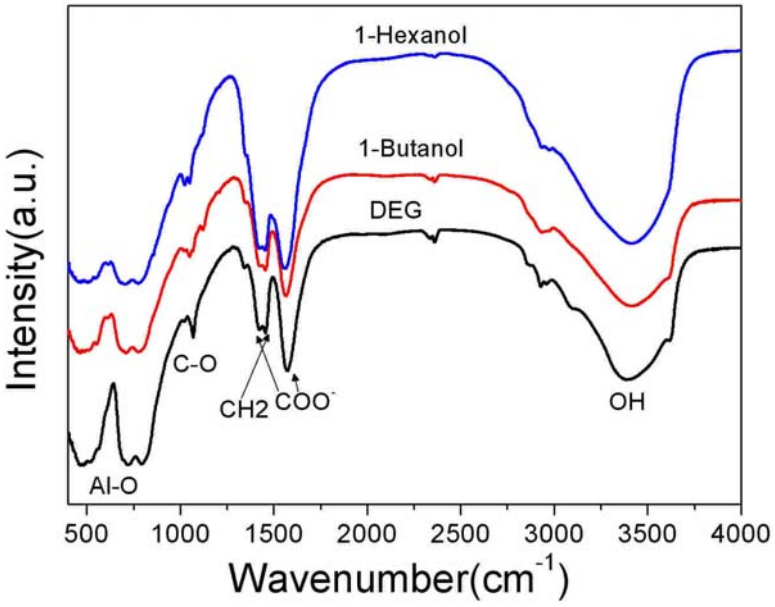

Figure S3: FTIR spectra of YAG samples obtained with solvents.

S4. The irradiation stability of the YAG:Ce(1%) colloids. Under irradiation of 450nm for 80 minutes, no intensity variation can be observed in this period.

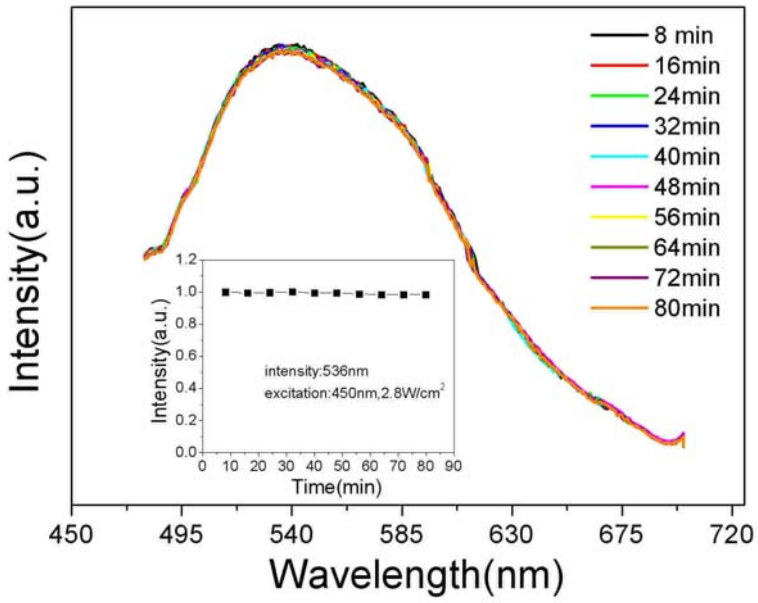

Figure S4. The irradiation stability of the YAG:Ce(1%) colloids dispersed in water with a concention of 2.5mg/ml. The excitation position is 450nm with a powerdensity of 28 mW/cm^2 from xenon lamp and the whole time was 8 minutes. Inset: The corresponding intensity of the emissions monitoring 536nm in this measuring peroid.

S5 BC-37 cell imaging. The imaging function of these NPs were also confirmed with another cancerous cell BC-37, which indicates the non-specific imaging property of the YAG:Ce NPs.

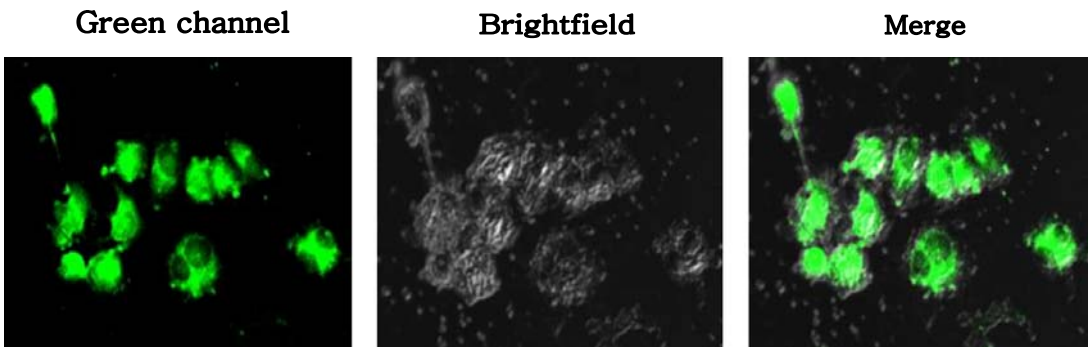

Figure S5. Confocal, bright field, and superimposed images of live BCap-37 cells labeled with YAG:Ce NPs. The images are false colored.